Physica B 407 (2012) 3252–3255

Contents lists available at SciVerse ScienceDirect

Physica B

journal homepage: www.elsevier.com/locate/physb

Influence of the spin–orbit interaction in the impurity-band states of n-doped semiconductors

G.A. Intronati [a,b,c,*], P.I. Tamborenea [a,b], D. Weinmann [b], R.A. Jalabert [b]

[a] Depto. de Física and IFIBA, FCEN, U. de Buenos Aires, Ciudad Universitaria, Pab. I, C1428EHA Buenos Aires, Argentina
[b] IPCMS, UMR 7504, CNRS-UdS, 23 rue du Loess, BP 43, 67034 Strasbourg Cedex 2, France
[c] Service de Physique de l'État Condensé, CNRS URA 2464, CEA Saclay, 91191 Gif-sur-Yvette, France

ARTICLE INFO

Available online 5 January 2012

Keywords:
Semiconductors
Impurity band
Metal–insulator transition
Spin relaxation

ABSTRACT

We study numerically the effects of an extrinsic spin–orbit interaction on the model of electrons in n-doped semiconductors of Matsubara and Toyozawa (MT). We focus on the analysis of the density of states (DOS) and the inverse participation ratio (IPR) of the spin–orbit perturbed states in the MT set of energy eigenstates in order to characterize the eigenstates with respect to their extended or localized nature. The finite sizes that we are able to consider necessitate an enhancement of the spin–orbit coupling strength in order to obtain a meaningful perturbation. The IPR and DOS are then studied as a function of the enhancement parameter.

The metal–insulator transition (MIT) is one of the paradigms of Condensed Matter Physics [1,2] and new features constantly appear according to the physical properties under study, the specific system or the emerging experimental techniques. The richness of the physics around the MIT stems from the fact that it is a quantum phase transition where disorder and Coulomb interactions coexist and compete in the determination of the ground state. In the case of the n-doped semiconductors, the MIT appears at doping densities where the Fermi level is in the impurity band [3,4]. This observation allows a description taking into account only the electronic states built from the hydrogenic ground state of the doping impurities. For densities slightly larger than the critical one (in the metallic side of the transition) non-interacting models, like the Matsubara–Toyozawa (MT) [5], are applicable. Furthermore, the previous description in terms of impurity sites is often traded by the Anderson model of a tight-binding lattice with on-site or hopping disorder. Large amounts of numerical work have been devoted to the Anderson model [6] and the critical exponents obtained fit reasonably well those of the experimental measurements [7].

The recently developed field of spintronics is contributing to put the MIT again into the focus of the condensed matter community. A key concept for possible applications of spintronics is the spin relaxation time, that is, the typical time in which the electron spin loses its initially prepared direction. Interestingly, the maximum spin relaxation times in n-doped semiconductors have been observed for impurity densities close to that of the MIT [8–11]. This intriguing physics is not completely understood at present, and various mechanisms of spin relaxation have been thought to be active at the MIT region [12–15]. At the level of models, the generalization of the Anderson model in order to include some spin–orbit coupling has been provided by Ando [16]. While this model is very useful to study the progressive breaking of the spin symmetry [17], its connection with experimentally relevant systems requires the estimation of coupling parameters which are not obtainable from first principles. This situation has led us to reconsider the MT model of impurity sites randomly placed in order to incorporate into the spin–orbit interaction. The various spin–orbit couplings (intrinsic and extrinsic) can be included and lead to effective Hamiltonians which depend on fundamental material constants, rather than on adjustable parameters.

In this paper we first consider the MT model in order to characterize the regions of extended and localized states, analyzing the limitations of the model and the conditions of applicability. We then include one of the sources of spin–orbit coupling, i.e. the interaction arising from the electrostatic potential of the impurities [15]. This extrinsic mechanism is analogous to the well-known Rasbha coupling generated in low-dimensional systems by the effect of an electrostatic asymmetric confining potential. We then study how the previously studied character of the MT eigenstates evolves under increasing values of the spin–orbit coupling strength. This work is a necessary step toward the understanding of spin dynamics in the generalized models that will allow us to extract the spin relaxation times close to the MIT.

We start by considering the MT Hamiltonian [5]

$$\mathcal{H}_0 = \sum_{m \neq m',\sigma} t^{\sigma\sigma}_{m'm} c^{\dagger}_{m'\sigma} c_{m\sigma}, \tag{1}$$

* Corresponding author at: Depto. de Física and IFIBA, FCEN, U. de Buenos Aires, Ciudad Universitaria, Pab. I, C1428EHA Buenos Aires, Argentina.
E-mail address: gintro@df.uba.ar (G.A. Intronati).

0921-4526/$ - see front matter © 2012 Elsevier B.V. All rights reserved.
doi:10.1016/j.physb.2011.12.079

where $c^{\dagger}_{m'\sigma}$ ($c_{m\sigma}$) represents the creation (annihilation) operator for the ground state of the impurity at site m' (m) with spin projection σ in the z-direction. The spin degree of freedom is irrelevant for the MT model, but it will become crucial later. The hopping matrix element is

$$t^{\sigma\sigma}_{m'm} = \langle \phi_{m'} | V_{m'} | \phi_m \rangle = -V_0 \left(1 + \frac{R_{m'm}}{a}\right) \exp\left(-\frac{R_{m'm}}{a}\right), \tag{2}$$

where $\phi_p(\mathbf{r}) = \phi(|\mathbf{r}-\mathbf{R}_p|)$, with $\phi(\mathbf{r}) = 1/(\pi a^3)^{1/2} \times \exp(-r/a)$, and a is the effective Bohr radius. The Coulombic potential produced by the impurity placed at $\mathbf{R}_p$ is $V_p(\mathbf{r}) = -V_0(a/|\mathbf{r}-\mathbf{R}_p|)$, where $V_0 = e^2/\varepsilon a$ and ε stands for the static dielectric constant of the semiconductor.

In order to characterize the electronic eigenstates in the impurity band from the point of view of their extended or localized nature, we obtain numerically the eigenvalues and eigenstates $\{\varepsilon_i, \psi_i\}$ of $\mathcal{H}_0$ for given configurations in which N impurities are randomly placed in a three-dimensional volume. For each configuration we calculate the energy-dependent density of states

$$\mathrm{DOS} = \sum_i \delta(\varepsilon - \varepsilon_i) \tag{3}$$

and the inverse participation ratio of the state $|\psi_i\rangle$

$$\mathrm{IPR} = \left[\frac{\sum_m |\langle \phi_m | \psi_i \rangle|^4}{(\sum_m |\langle \phi_m | \psi_i \rangle|^2)^2} \right]^{-1}. \tag{4}$$

In Fig. 1 we present the impurity-averaged DOS and IPR for three densities on the metallic side of the transition. The impurity band develops around the $E=0$ level of the isolated impurity in an asymmetric fashion: the DOS exhibits a long low-energy tail while the high-energy part is bounded by $E=1$ (in units of V_0). We verify that the width of the impurity band increases with the doping density. The numerically obtained DOS for different densities are well reproduced by approximate methods like diagrammatic perturbation [5] or moment expansion [18]. The highest energy states correspond to electronic wave functions localized on small clusters of impurities. This clustering is known to happen in realistic systems due to the lack of hard-core repulsion between impurities on the scale of a [19,15].

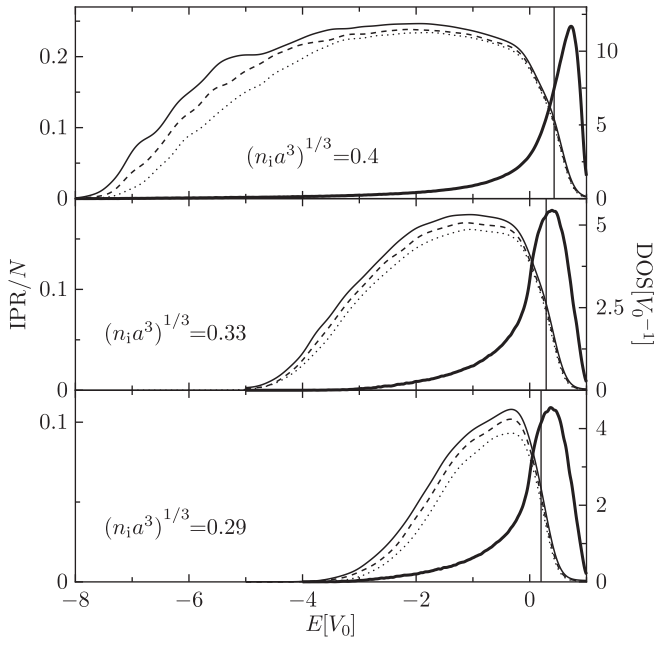

Fig. 1. Density of states (DOS, thick line and right scale) and inverse participation ratio (IPR, left scale) for three different densities on the metallic side of the metal–insulator transition, obtained through impurity averaging in the Matsubara–Toyozawa model. The solid, dashed and dotted curves of IPR/N are for N=2744, 4096 and 5832, respectively, and the vertical lines indicate the Fermi energy.

Before continuing with the analysis of the numerical results obtained from the MT model, we discuss some technical features of the model and the difficulties that we face in trying to improve upon it. Firstly, we notice that the chosen basis set is not orthogonal. In principle, we can deal with this issue by writing a generalized eigenvalue problem which includes the matrix of orbital overlaps [20,21]. This procedure results in unphysical high-energy states (with $E \gg 1$) that necessitate the inclusion of hydrogenic states beyond the 1s orbital in order to be described properly. However, care must be taken since enlarging the basis set leads to the problem of overcompleteness. Fortunately, for the properties we are interested in, the effects arising from non-orthogonality are known to be small for moderate doping densities, and that is why we will not consider them in the numerical work, thus staying within the original MT model. Finally, another drawback of the MT model is that the high-energy edge of the impurity band overlaps with the conduction band, which starts at $V_0/2$ (the effective Rydberg) and is not included in the MT description. As seen in Fig. 1 the DOS beyond $V_0/2$ is always very small, and therefore we can ignore the effects that the hybridization of the bands would yield in a more complete model.

The determination of the mobility edges from the size scaling of Fig. 1 is not straightforward. This difficulty arises from the heavily structured DOS of the MT model [21]. At low energy the small values of the DOS translate into a poor statistics for feasible sizes. In the high-energy part of the impurity band, the separation between the curves corresponding to different values of N is masked by the small values of the IPR/N.

For the highest density (top panel) the IPR/N exhibits a relatively flat region at intermediate energies, which is approximately independent of N for the two largest system sizes. The lower mobility edge can be located roughly at $E \sim 3.5$, where the latter curves separate. For lower impurity densities (lower panels) the previous analysis becomes increasingly demanding in terms of system sizes. We see that the flat region of IPR/N shrinks from which we can conclude that the lower mobility edge is shifting toward higher values of E.

The study of spin relaxation in doped semiconductors with densities close to that of the MIT calls for a generalization of the previously discussed MT model that incorporates spin–orbit coupling. Such an extension was done in Ref. [15], where a spin-flip term

$$\mathcal{H}_1 = \sum_{m \neq m', \sigma} t^{\sigma\overline{\sigma}}_{m'm} c^{\dagger}_{m'\overline{\sigma}} c_{m\sigma} \tag{5}$$

was added to $\mathcal{H}_0$ ($\overline{\sigma} = -\sigma$). Similar to the spin-conserving case, we have

$$t^{\sigma\overline{\sigma}}_{m'm} = \sum_{p \neq m} \langle \tilde{\psi}_{m'\overline{\sigma}} | V_p | \tilde{\psi}_{m\sigma} \rangle. \tag{6}$$

The wave function $\tilde{\psi}_{m\sigma}$ is an impurity spin-admixed (ISA) state with an envelope part $\phi_m(\mathbf{r})$ and a lattice-periodic part (conduction band) which has a small spin admixture. In Ref. [15], the expression of the matrix elements of Eq. (6) within an 8-band Kane model has been obtained. Here, we evaluate the three-center matrix elements numerically.

Spin–orbit coupling is known to favor the delocalization of disordered systems in two dimensions. In what follows we repeat the previous analysis, performed on the MT model, for its spin–orbit generalized counterpart.

The matrix element (6) is proportional to the effective spin–orbit coupling λ which for a zinc-blende semiconductor can be orders of magnitude larger than the one of vacuum $\lambda_0 \simeq 3.7 \times 10^{-6}$ Å^2. For the case of GaAs treated in Ref. [15], $\lambda \simeq -5.3$ Å^2 [22]. Still, the

spin-admixture perturbation energies are, even for largest system sizes that we can treat numerically, orders of magnitude smaller than the MT level spacing. We are then led to consider an enhancement factor R_r that multiplies λ and makes the two previous energy scales comparable. In Fig. 2 we show the spectral decomposition of a MT eigenstate with $\sigma=1$ on the basis of spin-admixed eigenstates of $\mathcal{H}_0+\mathcal{H}_1$. Only for enhanced values of R_r we do obtain significant projections into the two spin-admixed subspaces. The study of larger values of R_r then appears not only as a useful tool for analyzing the progressive inclusion of spin–orbit effects, but also as a need for numerical simulations of the spin dynamics.

In Fig. 3 we present the DOS and IPR/N of the extended model for the three densities previously treated and various values of the spin–orbit coupling strength R_r. Since the eigenstates of the full Hamiltonian are no longer spin eigenstates, the IPR should be calculated by projecting the state onto each impurity orbital including both spin orientations, that is

$$\mathrm{IPR}=\left[\frac{\sum_m(\sum_\sigma|\langle\phi_m\sigma|\psi_i\rangle|^2)^2}{(\sum_{m,\sigma}|\langle\phi_m\sigma|\psi_i\rangle|^2)^2}\right]^{-1}. \tag{7}$$

The DOS does not noticeably change with R_r, and that is why we only present the $R_r=1$ case. The spin–orbit coupling results in the increase of the IPR/N as a function of R_r in the region of extended states. This effect is more prominent for the larger density. The low-energy sector that has localized states in the MT model exhibits IPR/N curves approximately independent of N, which is a signature of the delocalization tendency.

We also performed a finite-size scaling of the IPR/N for a given density above the MIT critical density and one value of the spin–orbit coupling enhancement factor, $R_r=50$. It turns out that the relative insensitivity of IPR/N with N implies that the lower mobility edge has considerably shifted toward lower energy.

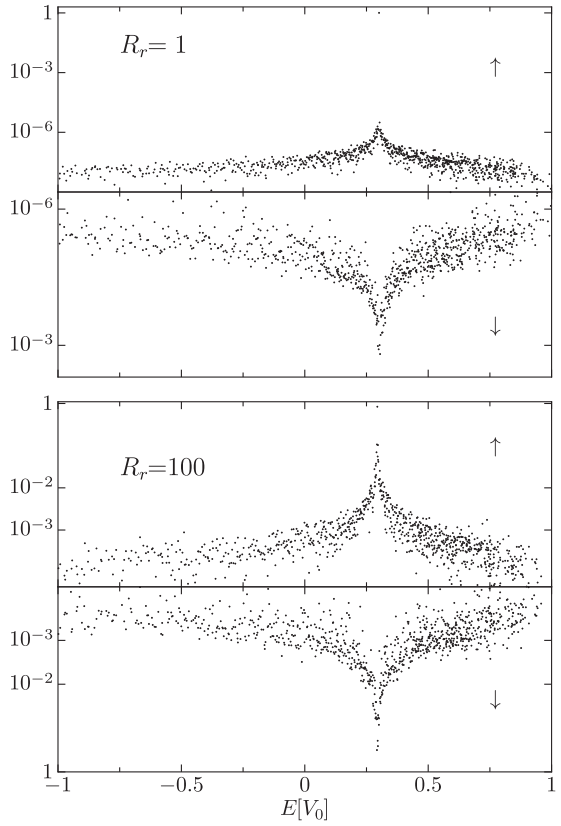

Fig. 2. Spectral decomposition of a Matsubara–Toyozawa eigenstate into the basis set formed by the eigenstates of the spin–orbit extended model. The system size is $N=1000$ and the density is given by $(n_ia^3)^{1/3}=0.33$. Top and bottom panels correspond to $R_r=1$ and 100, respectively.

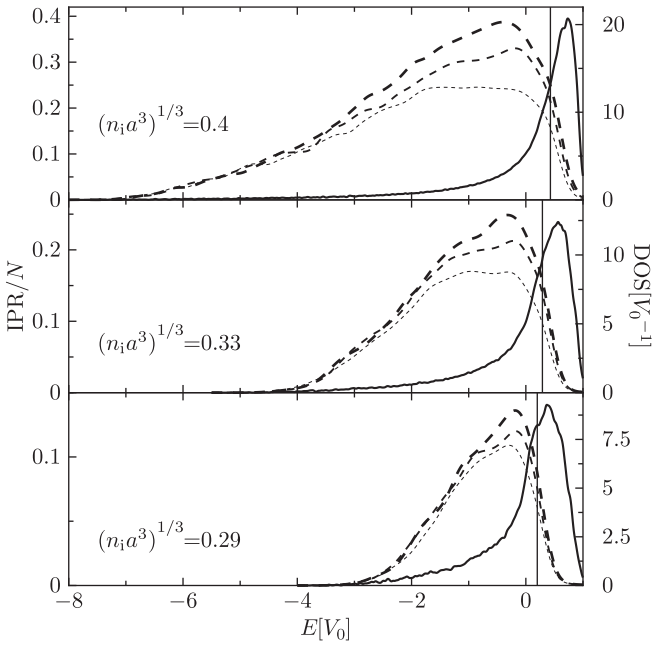

Fig. 3. Density of states (DOS, solid line and right scale) and inverse participation ratio (IPR, dashed lines and left scale) for three different densities on the metallic side of the metal–insulator transition. Dashed lines with increasing thickness are for $R_r=50$, 150 and 250, respectively. The vertical lines indicate the Fermi energy.

In conclusion, we revisited the problem of the characterization of the eigenstates of the Matsubara–Toyozawa model from the point of view of their localization, and performed a similar analysis in an extended model proposed recently which includes the extrinsic spin–orbit coupling mechanism arising from the electrostatic potential of the hydrogenic impurities. Analyzing the effect of spin–orbit coupling of various strengths is necessary in order to address the study of the spin dynamics in the impurity band of doped semiconductors. We found that while the density of states is not considerably modified by the spin–orbit interaction, the nature of the states is noticeably affected by it showing a tendency to the delocalization.

Acknowledgments

We acknowledge the financial support from the ANR through Grant ANR-08-BLAN-0030-02, the Collège Doctoral Européen of the Université de Strasbourg, UBACYT through Grant number X495, the ANPCyT through Grant PICT 2006-02134, the program ECOS-Sud (action A10E06), and the Marie Curie ITN through NanoCTM (contract 234970).

References

[1] N. Mott, Conduction in Non-crystalline Materials, Oxford Science Publications, Clarendon Press, Oxford, 1987.
[2] F. Gebhard, The Mott Metal Insulator Transition: Models and Methods, Springer, Berlin, 2010.
[3] B.I. Shklovskii, A.L. Efros, Electronic Properties of Doped Semiconductors, Springer Verlag, New York, Tokyo, 1984.
[4] E.N. Economou, A.C. Fertis, in: H. Fritzsche, D. Adler (Eds.), Localization and Metal–Insulator Transitions, Plenum Press, New York, 1985.
[5] T. Matsubara, Y. Toyozawa, Prog. Theor. Phys. 26 (1961) 739.
[6] B. Kramer, A. MacKinnon, Rep. Prog. Phys. 56 (1993) 1469.
[7] B. Kramer, et al., Int. J. Mod. Phys. 24 (2010) 1841.
[8] V. Zarifis, T.G. Castner, Phys. Rev. B 36 (1987) 6198.
[9] J.M. Kikkawa, D.D. Awschalom, Phys. Rev. Lett. 80 (1998) 4313.
[10] R.I. Dzhioev, et al., Phys. Rev. B 66 (2002) 245204.

[11] M. Römer, et al., Phys. Rev. B 81 (2010) 075216.
[12] B.I. Shklovskii, Phys. Rev. B 73 (2006) 193201.
[13] K.V. Kavokin, Phys. Rev. B 64 (2001) 075305.
[14] W.O. Putikka, R. Joynt, Phys. Rev. B 70 (2004) 113201.
[15] P.I. Tamborenea, D. Weinmann, R.A. Jalabert, Phys. Rev. B 76 (2007) 085209.
[16] T. Ando, Phys. Rev. B 40 (1989) 5325.
[17] Y. Asada, K. Slevin, T. Ohtsuki, Phys. Rev. Lett. 89 (2002) 256601.
[18] J.-P. Gaspard, F. Cyrot-Lackmann, J. Phys. C 6 (1973) 3077.
[19] G.A. Thomas, et al., Phys. Rev. B 23 (1981) 5472.
[20] N. Majlis, E. Anda, J. Phys. C: Solid State Phys. 11 (1978) 1607.
[21] W.Y. Ching, D.L. Huber, Phys. Rev. B 26 (1982) 5596.
[22] R. Winkler, Spin–Orbit Coupling Effects in Two-dimensional Electron and Hole Systems, Springer-Verlag, Berlin, 2003.